Available online at www.sciencedirect.com
ScienceDirect
Journal of Power Sources 176 (2008) 183–190
JOURNAL OF POWER SOURCES
www.elsevier.com/locate/jpowsour

A self-regulated passive fuel-feed system for passive direct methanol fuel cells

Y.H. Chan, T.S. Zhao *, R. Chen, C. Xu

Department of Mechanical Engineering, The Hong Kong University of Science and Technology, Clear Water Bay, Kowloon, Hong Kong SAR, China

Received 20 September 2007; received in revised form 14 October 2007; accepted 15 October 2007
Available online 24 October 2007

Abstract

Operating a passive direct methanol fuel cell (DMFC) with high methanol concentration is desired because this increases the energy density of the fuel cell system and hence results in a longer runtime. However, the increase in methanol concentration is limited by the adverse effect of methanol crossover in the conventional design. To overcome this problem, we propose a new self-regulated passive fuel-feed system that not only enables the passive DMFC to operate with high-concentration methanol solution without serious methanol crossover, but also allows a self-regulation of the feed rate of methanol solution in response to discharging current. The experimental results showed that with this fuel-feed system, the fuel cell fed with high methanol concentration of 12.0 M yielded the same performance as that of the conventional DMFC running with 4.0 M methanol solution. Moreover, as a result of the increased energy density, the runtime of the cell with this new system was as long as 10.1 h, doubling that of the conventional design (4.4 h) at a given fuel tank volume. It was also demonstrated that this passive fuel-feed system could successfully self-regulate the fuel-feed rate in response to the change in discharging currents.

Keywords: Passive direct methanol fuel cell (DMFC); Passive fuel-feed system; Methanol crossover

1. Introduction

Direct methanol fuel cells (DMFCs) have been recognized as the most promising candidate to replace conventional batteries for powering portable electronic devices, such as laptops, cellular phones and personal digital assistants (PDAs), because of its unique advantages of high energy density, low emission and ease in handling the fuel. Over the past decade, extensive efforts have been exerted on the study of the active DMFCs with the fuel fed by a liquid pump and oxidant fed by a gas compressor [1–5]. However, for portable applications, it is desired that the parasitic energy losses caused by the fuel cell ancillary devices, such as methanol fuel supply devices, air blowers, heat exchangers, etc. be minimized or eliminated such that the energy density and efficiency of the fuel cell system can be increased. Therefore, various DMFC systems that operate under passive conditions, i.e., air breathing and passive methanol supply, have been proposed and studied [6–18]. These types of fuel cell not only offer the advantage of simplicity and more compact system but also make it possible to eliminate the parasitic power losses for powering ancillary devices required in active DMFCs. Because of these advantages, the passive DMFC has become much more attractive.

Presently, one of the most challenging problems for the DMFCs (both active and passive) that employ Nafion membranes is methanol crossover from the anode to the cathode, which causes a mixed potential on the cathode and thus reduces the overall cell voltage. Because of this, low methanol concentrations are usually used to achieve a desirable cell performance. However, a low methanol concentration leads to a low energy density of the fuel cell system and thus a short runtime, which cannot meet the requirement of the commercialization. Hence, some researchers [19–25] made their efforts on the fuel delivery system to increase the feed methanol concentration. Abdelkareem et al. [19–21] investigated the effect of employing a porous carbon plate on the performance of a passive DMFC and found that high methanol concentration solution could be used because of the increased mass-transfer resistance on the anode resulting

* Corresponding author. Tel.: +86 852 2358 8647; fax: +86 852 2358 1543.
E-mail address: metzhao@ust.hk (T.S. Zhao).

0378-7753/$ – see front matter © 2007 Elsevier B.V. All rights reserved.
doi:10.1016/j.jpowsour.2007.10.050

from the porous carbon plate. Kim et al. [22–23] employed hydrogels in methanol fuel cartridges to control methanol diffusion rate from the fuel reservoir to the anode electrode. Their experimental results implied that the hydrogel retards methanol transfer rate, even at high methanol concentrations, and thus suppresses the rate of methanol crossover, resulting in a higher methanol concentration operation. Recently, Kim [24] proposed a vapor-feed DMFC to achieve a high energy density by using pure methanol for mobile applications. In his work, a multi-layered porous structure consisting of vaporizer, barrier and buffer layer were introduced on the anode, which cannot only vaporize the methanol but also increase the mass-transfer resistance. Yang and Liang [25] divided the fuel tank into two parts: one water tank and one pure methanol tank. By adding a hydrophobic porous layer between the water tank and pure methanol tank to increase the methanol transfer resistance, the pure methanol can be used without suffering from serious methanol crossover.

Our literature review indicates that most previous research works about fuel delivery method are to add the porous material on the anode to increase the methanol transfer resistance, leading to the high methanol concentrations or even pure methanol operation with low methanol crossover. In this work, a self-regulated passive fuel-feed system driven by the exhausted gas CO_2 is proposed for the passive DMFC. With this system, the high methanol concentration solution is supplied to the anode reaction chamber in response to the methanol consumption rate, while the methanol concentration in the anode reaction chamber is maintained at a low level to suppress the methanol crossover. The experimental results demonstrated that the passive DMFC with the proposed new fuel-feed system can successfully operate at high methanol concentration of 12.0 M for 10.1 h, which is much longer than that of the conventional design.

2. Conceptual design

The passive fuel-feed system is conceptually shown in Fig. 1, which consists of a reaction chamber, a fuel tank with a built-in spring, a fuel-feed valve and a pressure release valve. Dilute methanol solution is stored in the reaction chamber, while high methanol concentration solution is stored in the fuel tank. The fuel cell operates with the dilute methanol solution stored in the reaction chamber. The consumed methanol in the reaction chamber is made up by the high methanol concentration solution in the fuel tank. The feed rate from the fuel tank to the reaction chamber is controlled by the gas CO_2 generation rate, which is proportional to current density. This control process is achieved by the above-mentioned two valves, which are automatically regulated by the gas pressure inside the reaction chamber. As such, the methanol concentration in the reaction chamber can be maintained at a desired level during the discharging process. The working principle of the fuel-feed system can be detailed by referring to the operation flow chart shown in Fig. 2. At the beginning, both the pressure release valve and fuel-feed valve are closed, meaning that the reaction chamber is initially sealed. When the fuel cell discharges, the gas CO_2 is produced at the anode and flows to the sealed reaction chamber. As a result, the pressure in the reaction chamber increases with time. Once the pressure reaches a certain value P_1, both the fuel-feed valve and the pressure release valve are open. Subsequently, the fuel in the fuel tank is fed into the reaction chamber as a result of the driving force from the spring, while the accumulated gas CO_2 in the reaction chamber is released to the ambient. The discharge of the gas CO_2 from the reaction chamber causes the pressure to decrease. At a sufficiently low pressure both the valves are closed and the gas CO_2 starts to build up again, completing a working cycle. As such, the high methanol concentration solution is periodically fed into the reaction chamber and the feed rate depends on the gas CO_2 generation rate, which is proportional to current density. When the current density is increased, more methanol will be consumed due to the electrochemical reaction and the generation rate of gas CO_2 is also increased, leading to a quicker increase in the pressure inside the reaction chamber. As a consequence, the open–close period of both the valves becomes shorter, resulting in a higher feed

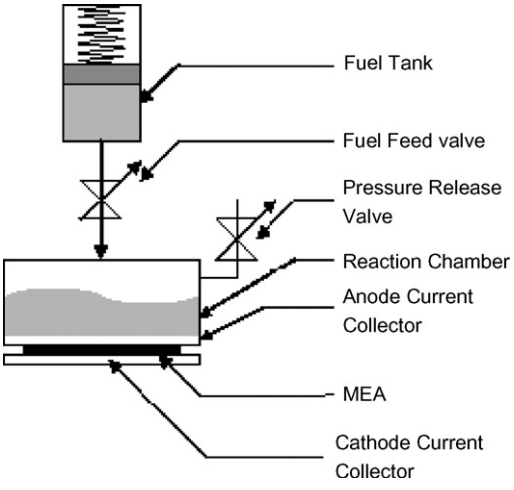

Fig. 1. Schematic of the passive DMFC with the passive fuel-feed system.

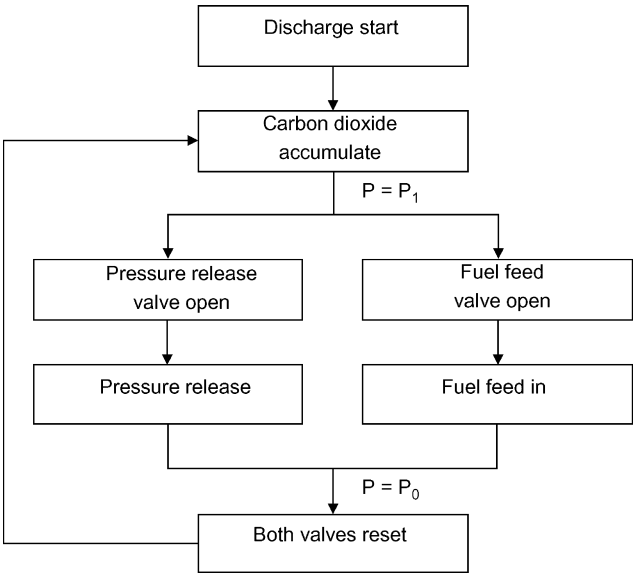

Fig. 2. Operation flow chart of the passive fuel-feed system.

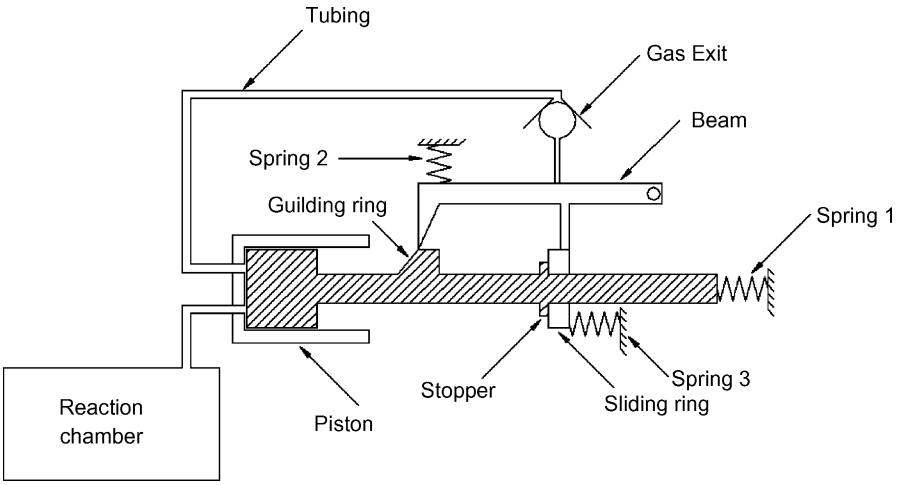

Fig. 3. Schematic of the pressure release valve.

rate. Hence, the passive fuel-feed system can self-regulate the feed rate in response to a change in the discharging current of the fuel cell. More importantly, since this design of the passive fuel-feed system allows high-concentration methanol solution to be supplied to the fuel cell system, the energy density of the fuel cell system is high and hence the fuel cell runtime can be highly increased. The successful operation of this passive fuel-feed system depends on the two key components: the pressure release valve and fuel-feed valve, which are detailed as follows.

2.1. Pressure release valve

This key component not only controls the maximum gas pressure, P_1, in the reaction chamber to release the accumulated gas CO_2, but also prevents air from entering the chamber. Hence, the pre-set release pressure, P_1, controls the fuel-feed rate. Fig. 3 shows the conceptual design of the pressure release valve, which consists of five major components: a piston with a guiding ring and a stopper, a sliding ring, three springs, a beam and a gas exit. The working principle of the pressure release valve can be explained by referring to Fig. 4, in which the entire valve open–close cycle is divided into four stages. At the stage 1, the pressure inside the reaction chamber is set to be P_0, which is slightly higher than the atmospheric pressure. The gas exit is shut-off by the beam, which is supported by the sliding ring. At the stage 2, the generated gas CO_2 accumulates in the reaction chamber, leading to an increase in the gas pressure. The increased pressure pushes the piston, together with the stopper to move right. The stopper pushes the sliding ring rightward. During this stage, the beam is still held by the sliding ring. Hence the gas exit remains at the shut-off status. With the pressure further increasing to P_1, the pressure release valve enters the stage 3, where the beam loses the support from the sliding ring and is pushed down by the spring 2, leading to the open of the gas exit. Thus the gas CO_2 in the reaction chamber is released to the ambient, which leads to the drop in the pressure. At the stage 4, the piston together with the guiding ring is pushed back by the spring 1 because of the reduced pressure in the reaction chamber and the beam is also raised. Once the piston and beam are restored to the original position, the sliding ring can hold the beam again and thus the gas exit is shut-off, forming an open–close cycle.

2.2. Fuel-feed valve

This component controls the feed rate of high-concentration methanol solution into the reaction chamber. The fuel-feed valve is closed when the pressure inside the reaction chamber is lower than P_1. Once the pressure increases to P_1, this valve is opened and the high-concentration methanol solution is fed into the reaction chamber by the spring as shown in Fig. 1. After the gas CO_2 is released, the pressure is reduced and the fuel-feed valve is shut-off.

It should be mentioned that since the above-described fuel-feed system is driven by the exhausted gas CO_2 from the DMFC, the system is sensitive to the cell orientation. A previous experimental study [6] revealed that the orientation with the anode facing downward would result in extremely unstable operation as a large number of CO_2 bubbles were accumulated at the anode catalyst layer due to buoyancy force, which blocked the methanol transport toward the anode catalyst layer. Hence, in this work the horizontal orientation with the anode facing upward is only considered.

3. Theoretical analysis

Prior to testing the passive DMFC with the new fuel-feed system, we make an approximate analysis of the methanol feed rate and cycling time for the system design and operation. For simplicity we consider the mass balance of methanol only but ignore water transport and loss at the anode. According to the mass balance, the methanol consumption rate is equal to the methanol flux from the reaction chamber to the anode catalyst layer (ACL), which can be expressed as

$$\dot{M}_{\mathrm{MeOH}} = \frac{A_{\mathrm{cell}}(c_{\mathrm{MeOH,chamber}} - c_{\mathrm{MeOH,ACL}})}{\delta_{\mathrm{CC}}/\varepsilon_{\mathrm{CC}} D_{\mathrm{MeOH,l}} + \delta_{\mathrm{ADL}}/D_{\mathrm{MeOH,ADL}}} \quad (1)$$

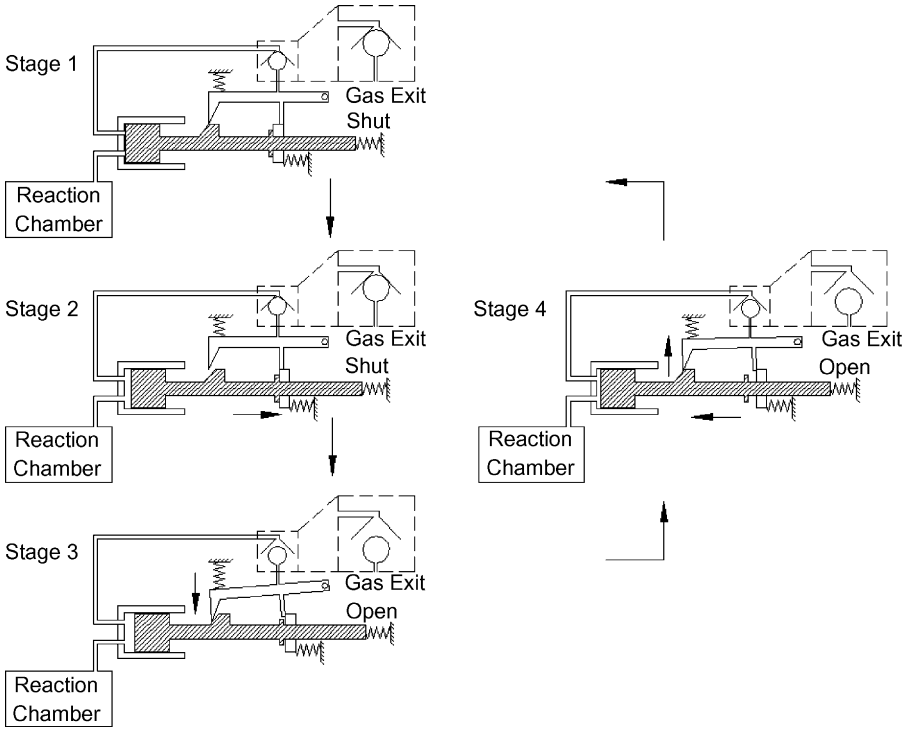

Fig. 4. Working principle of the pressure release valve.

where A_{cell} is the active surface area of membrane electrode assembly (MEA), ε_{CC} the open ration of current collector (CC), $c_{MeOH,chamber}$ and $c_{MeOH,ACL}$ represent the methanol concentration in the reaction chamber and the ACL, δ_{CC} and δ_{ADL} represent the thickness of the CC and the anode diffusion layer (ADL), $D_{MeOH,1}$ and $D_{MeOH,ADL}$ stand for the methanol diffusivity in the water and the effective methanol diffusivity in the ADL which can be expressed as $(\varepsilon_{ADL})^{3/2}D_{MeOH,1}$ with ε_{ADL} denoting the porosity of the ADL.

At the ACL, part of methanol is electrochemically oxidized to produce electrons, protons and gas CO_2, whereas the remainder is directly transported through the membrane to the cathode (methanol crossover). Thus the methanol consumption rate can be expressed by

$$\dot{M}_{MeOH} = \dot{M}_{MOR} + \dot{M}_{crossover} \tag{2}$$

where $\dot{M}_{MOR}$ is the consumption rate due to the methanol oxidation reaction (MOR) and $\dot{M}_{crossover}$ is the flux of methanol crossover. According to Faraday's law, $\dot{M}_{MOR}$ can be given by

$$\dot{M}_{MOR} = A_{cell}\frac{I}{6F} \tag{3}$$

where I is the current density and F is Faraday's constant. On the other hand, $\dot{M}_{crossover}$ can be approximated from the concentration difference between the anode and cathode catalyst layer

$$\dot{M}_{crossover} = -A_{cell}D_{MeOH,N}\frac{dc}{dz} = A_{cell}D_{MeOH,N}\frac{c_{MeOH,ACL}}{\delta_{PEM}} \tag{4}$$

where $D_{MeOH,N}$ is the effective diffusivity of methanol in the membrane and δ_{PEM} is the thickness of the membrane. Here we ignore the electro-osmotic effect because of the relatively small discharging current density in our test, and we assume that the methanol in the cathode catalyst layer (CCL) is completely depleted due to the fast reaction of methanol in the cathode. Combining Eqs. (1)–(4), we can easily obtain the methanol consumption rate $\dot{M}_{MeOH}$.

We now turn our attention to the cycling time, which depends on the gas CO_2 generation rate at a given pre-set release pressure. According to Faraday's law, the gas CO_2 generation rate $\dot{M}_{CO_2}$ can be given by

$$\dot{M}_{CO_2} = A_{cell}\frac{I}{6F} \tag{5}$$

Assuming that the gas CO_2 is ideal gas, the release pressure $P_{release}$ can be related to the gas CO_2 generation rate and the cycling time can be determined by

$$t_{cycle} = \frac{P_{release}V_{chamber}}{\dot{M}_{CO_2}RT} \tag{6}$$

where $V_{chamber}$ is the gas volume of the sealed space including the reaction chamber and tube, R is the universal gas constant and T is the temperature.

Thus, with the calculated methanol consumption rate and cycling time, the methanol feed rate in each cycle, as well as the total runtime of the fuel cell system, can be determined. Based on the properties given in Table 1, the estimations of the methanol consumption rate, gas CO_2 generation rate, cycling time, methanol feed rate in each cycle and total runtime corresponding to the current density of 50 mA cm^{-2} are given in Table 2.

Table 1
Physicochemical properties

Parameter	Value	Unit	Reference
T	300	K	
δ_{PEM}	0.0125	cm	
δ_{ADL}	0.035	cm	
δ_{CC}	0.1	cm	
ε_{ADL}	0.7	–	[27]
$D_{MeOH,1}$	$10^{-2-999.778/T}$	$cm^2\ s^{-2}$	[28]
$D_{MeOH,N}$	$4.9 \times 10^{-6}\ e^{[2436(1/333-1/T)]}$	$cm^2\ s^{-2}$	[29]
V_{gas}	23	cm^3	

4. Experimental

4.1. Membrane electrode assembly

A membrane electrode assembly (MEA) with the active area of 6.0 cm^2 was fabricated with single-side ELAT electrodes from ETEK in both anode and cathode. Both electrodes use carbon cloth (E-TEK, Type A) with 30 wt.% PTFE wet-proofing treatment as the backing layer. The catalyst on the anode is PtRu black (1:1 a/o) with the loading of 4.0 mg cm^{-2}, while on the cathode is 40 wt.% Pt on Vulcan XC-72 with the loading of 2.0 mg cm^{-2}. Furthermore, 0.8 mg cm^{-2} dry Nafion ionomer was coated onto the surface of each electrode. The pretreated Nafion 115 membrane was employed as the electrolyte. The pretreatment process included boiling the membrane in 5 vol% H_2O_2, washing in DI water, boiling in 0.5 M H_2SO_4 and washing in DI water for 1 h in each step. Finally, the MEA with the active area of 6.0 cm^2 was fabricated by hot pressing at 135 °C at 4.0 MPa for 3 min. More information about the MEA fabrication can be found elsewhere [26].

4.2. Cell fixture

As shown in Fig. 5, the MEA mentioned above was sandwiched between an anode and a cathode current collector, and the entire cell setup was then held together between an anode and a cathode fixture, both of which were made of transparent acrylic. A 12.0 ml reaction chamber was built in the anode fixture, which is sealed by the proposed passive feeding system. Both the anode and cathode current collectors were made of a perforated 316L stainless steel plate of 1.0 mm in thickness. A plurality of hexagonal holes was machined in both the current collectors, serving as the passages of fuel and oxidant, which resulted in an open ratio of 54.1%. A 200-nm platinum layer was sputtered onto the surface of the current collectors to reduce the contact resistance with the electrodes.

Table 2
Numerical data for the system discharging at 50 mA cm^{-2}

Parameter	Value
Methanol consumption rate	1.38×10^{-6} mol s^{-2}
CO_2 generation rate	5.18×10^{-7} mol s^{-2}
Cycling time	8.89 min
Fuel injection in each cycle	0.061 cc
Runtime with 2 cc 4 M + 4 cc 12 M methanol solution	11.2 h

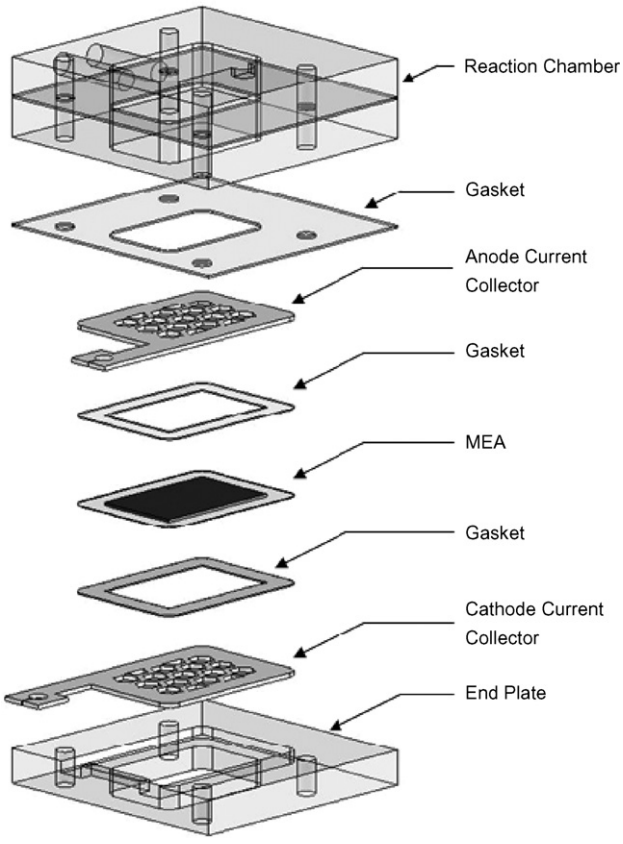

Fig. 5. Schematic of the cell fixture.

4.3. Electrochemical instrumentation and testing condition

An Arbin BT2000 electrical load interfaced to a computer was employed to control the condition of discharging and record the voltage–current curves. All the experiments of the passive DMFCs were performed at room temperature of 21–23 °C and with the relative humidity of 75–81%.

To test this fuel-feed system, 2.0 ml methanol solution of 4.0 M was fed into the reaction chamber at the beginning, while 4.0 ml methanol solution of 12.0 M was fed into the fuel tank. The pressure release valve was calibrated to open at the release pressure of 30 kPa.

5. Results and discussion

Fig. 6 compares the discharging voltage at the current density of 50 mA cm^{-2} for the passive DMFC with and without the fuel-feed system. Note that the fuel cell without the fuel-feed system was tested at the 4.0-M operation, as it has been shown that the cell could yield the highest performance at or near this particular methanol concentration [17,18]. It is seen that the cell with the fuel-feed system not only yielded a very stable cell voltage, which is almost the same as the conventional one at the 4.0-M operation, but also exhibited a much longer runtime

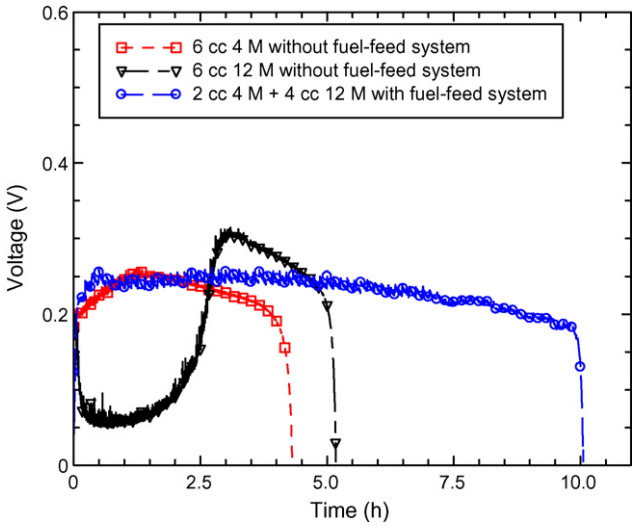

Fig. 6. Performance curve for the DMFCs with and without the passive fuel-feed system operated at current density of 50 mA cm^{-2}.

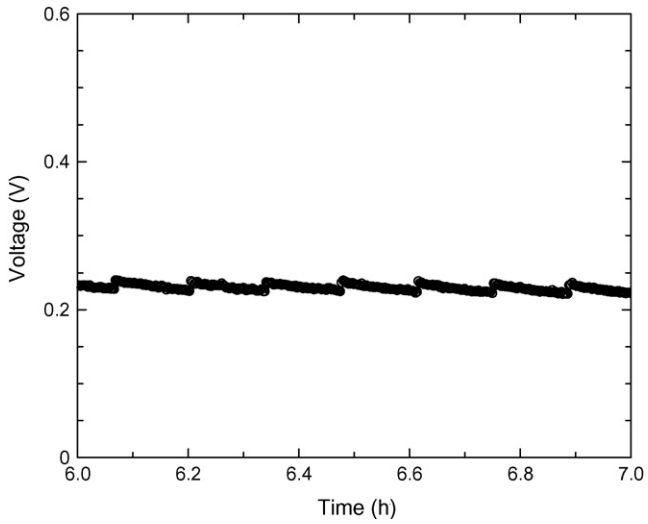

Fig. 7. Enlargement of performance curve for the DMFC with the fuel-feed system.

(10.1 h) than did the conventional one (4.4 h). The reason leading to these phenomena is explained as follows. As discussed in the previous section, although the high-concentration (12.0 M) methanol solution was supplied as the fuel, the methanol concentration in the reaction chamber was still maintained at about 4.0 M with the aid of the fuel-feed system. As a result, the cell with the fuel-feed system yielded a stable cell performance as did the 4.0 M conventional operation. Moreover, the high-concentration methanol solution (12.0 M) used for the passive DMFC can significantly increase the energy density of the fuel cell system, leading to a longer runtime. It should be noted that the practical runtime is slightly lower than the estimated value given in Table 2. This is possibly because the electro-osmotic effect on the methanol crossover was ignored in the estimation, resulting in an underestimated methanol consumption rate. To further demonstrate the advantage of the new fuel-feed system, we also tested the cell performance with the conventional design at the 12.0-M operation for comparison, as shown in Fig. 6. It can be found that although the conventional design at the 12.0-M operation had higher energy density than the cell with the fuel-feed system, the cell performance and runtime were much lower. This is because the methanol crossover was very severe for the conventional design at the 12.0-M operation, which caused poor performance and lower fuel efficiency, thereby a shorter runtime. In summary, these experimental results indicate that the passive DMFC with the new fuel-feed system can yield a stable and good performance with a long runtime at high methanol concentration operation without serious methanol crossover.

As mentioned above, the high-concentration methanol solution is fed from the fuel tank into the reaction chamber in each cycle according to the methanol consumption rate. To show this periodical behavior, the discharging voltage with the enlarged time scale is shown in Fig. 7. It is seen that the cell voltage is periodically varying with the time with the voltage variation of about 15 mV. It is believed that this voltage variation is caused by the pressure change inside the reaction chamber. When the pressure release valve is open at the pressure P_1, leading to a sudden removal of the CO_2 from the anode, the methanol transfer resistance from the chamber to the catalyst sites is reduced, which results in a jump in the cell voltage. The sudden removal of gas CO_2 from the anode can be evidenced by the captured bubble behavior shown in Fig. 8. It is seen from Fig. 8a that only a few bubbles were observed before the pressure release valve was open. However, once the pressure release valve was open, the CO_2 bubbles were easily removed from the ACL and ADL due to the lowered pressure, and a lot of bubbles were observed, as shown in Fig. 8b.

The cycling time of each cycle during the whole discharging process is shown in Fig. 9. It is seen that a stable cycling time of about 8 min was recorded, indicating that the fuel cell with this new fuel-feed system can operate rather stably. It is also found that the measured cycling time was slightly smaller

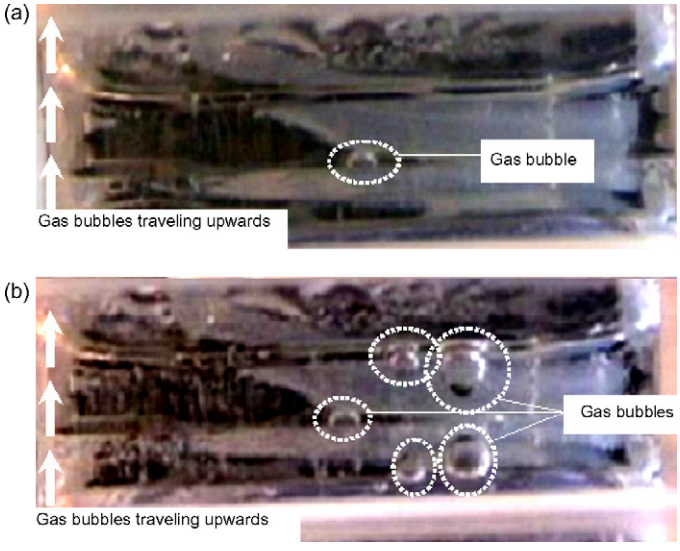

Fig. 8. (a) Before the open of pressure release valve inside the reaction chamber. (b) During the open of pressure release valve inside the reaction chamber.

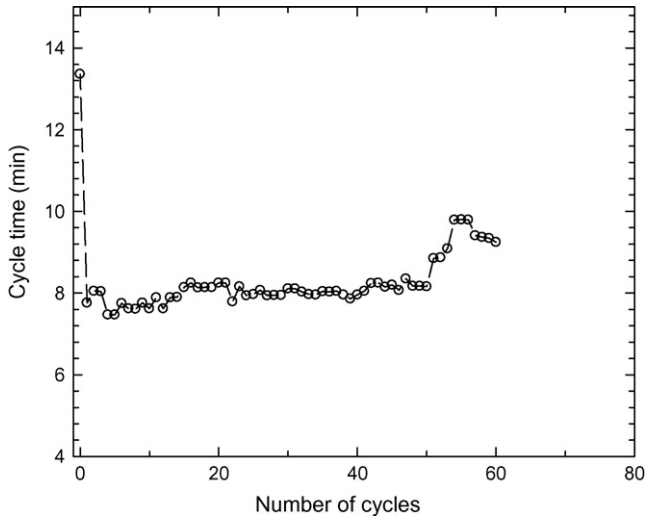

Fig. 9. Cycling time for the pressure release process operated at 50 mA cm^{-2}.

than the estimated value (8.89 min) given in Table 2. This is because the estimated value is obtained by assuming that the pressure in the reaction chamber is reduced to the atmospheric pressure after the gas release, which is lower than the real pressure P_0. This resulted in a reduction in the pressure difference between the beginning status and release status and thus a shorter cycling time for the practical operation. In addition, it is also found that the cycling time for the first cycle was much larger than the stable valve. This is because in the first cycle the gas CO_2 will not appear until the dilute methanol solution was saturated with the CO_2, while for all the following cycles the methanol solution was saturated with the CO_2 all the time. As such, the dissolving process of the CO_2 in the first cycle led to a much longer cycling time. In summary, the stable cycling time further demonstrates that with this new fuel-feed system, the passive DMFC can stably operate at high methanol concentration without suffering from serious methanol crossover.

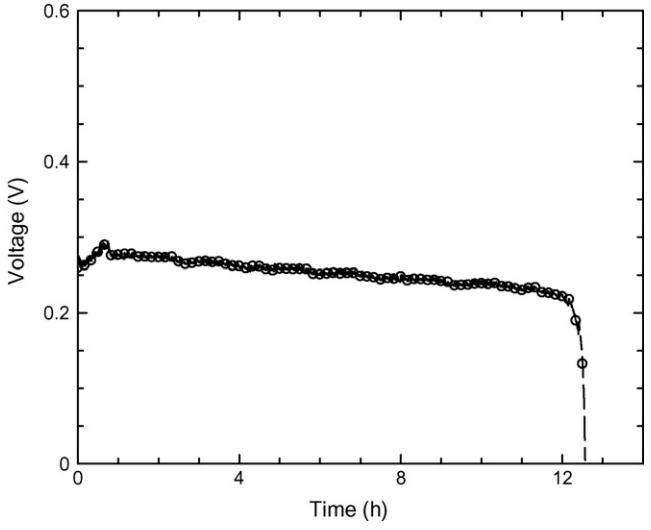

Fig. 10. The performance curve for the DMFCs with the passive fuel-feed system operated at 30 mA cm^{-2}.

Furthermore, as mentioned above, the new fuel-feed system can self-regulate the methanol feed rate in response to the discharging current density. Fig. 10 shows the discharging voltage of the fuel cell system at the current density of 30 mA cm^{-2}. It can be seen that the system successfully yielded a stable cell voltage for 14.5 h. The reduction in current density led to a lower methanol consumption rate and thereby a longer runtime. In addition, the cycling time of about 11.5 min was observed in the experiment which is larger than that of 50 mA cm^{-2} discharging because of the reduced CO_2 generation rate.

6. Concluding remarks

In this work, a self-regulated fuel-feed system for passive DMFCs was designed, fabricated and tested. This innovative fuel-feed system shows the following features: (i) use of high-concentration methanol solution; (ii) passive operation by utilizing the exhausted gas CO_2; (iii) self-regulation in response to discharging current density. It was found that the passive DMFC with this new feed system could operate at 12.0-M methanol solution without suffering from serious methanol crossover and yielded stable performance as compared to the conventional design. The high methanol concentration increases the energy density of the fuel cell system, resulting in a longer runtime of 10.1 h, which is almost twice larger than the conventional one. In addition, it is also revealed that this passive fuel-feed system can successfully self-regulate the feed rate in response to discharging current.

Acknowledgement

The work described in this paper was fully supported by a grant from the Research Grants Council of the Hong Kong Special Administrative Region, China (Project No. 622706).

References

[1] C.K. Dyer, J. Power Sources 106 (2002) 31.
[2] Q. Ye, T.S. Zhao, H. Yang, et al., Electrochem. Solid State Lett. 8 (2005) A52.
[3] X. Ren, T.E. Springer, T.A. Zawodzinski, et al., J. Electrochem. Soc. 147 (2000) 466.
[4] J. Prabhuram, T.S. Zhao, C.W. Wong, J.W. Guo, J. Power Sources 134 (2004) 1.
[5] Z. Qi, A. Kaufman, J. Power Sources 110 (2002) 177.
[6] R. Chen, T.S. Zhao, J.G. Liu, J. Power Sources 157 (2006) 351.
[7] Y.J. Kim, B. Bae, M.A. Scibioh, et al., J. Power Sources 157 (2006) 253.
[8] R. Chen, T.S. Zhao, Electrochim. Acta 52 (2007) 4317.
[9] H.K. Kim, J.M. Oh, J.H. Kim, H. Chang, J. Power Sources 162 (2006) 497.
[10] J.G. Liu, T.S. Zhao, Z.X. Liang, et al., J. Power Sources 153 (2006) 61.
[11] B.K. Kho, B. Bae, M.A. Scibioh, et al., J. Power Sources 142 (2005) 50.
[12] R. Chen, T.S. Zhao, Electrochem. Commun. 9 (2007) 718.
[13] T. Shimizu, T. Momma, M. Mohamedi, et al., J. Power Sources 137 (2004) 277.
[14] J. Han, E.S. Park, J. Power Sources 112 (2002) 477.
[15] C.Y. Chen, P. Yang, J. Power Sources 123 (2003) 37.
[16] J.J. Martin, W.M. Qian, H.J. Wang, et al., J. Power Sources 164 (2007) 287.
[17] J.G. Liu, T.S. Zhao, R. Chen, et al., Electrochem. Commun. 7 (2005) 288.
[18] R. Chen, T.S. Zhao, J. Power Sources 152 (2005) 122.

[19] M. Ali Abdelkareem, N. Nakagawa, J. Power Sources 162 (2006) 114.
[20] N. Nakagawa, M. Ali Abdelkareem, K. Sekimoto, J. Power Sources 160 (2006) 105.
[21] M. Ali Abdelkareem, N. Nakagawa, J. Power Sources 165 (2007) 685.
[22] W.J. Kim, H.G. Choi, Y.K. Lee, et al., J. Power Sources 163 (2006) 98.
[23] W.J. Kim, H.G. Choi, Y.K. Lee, et al., J. Power Sources 157 (2006) 193.
[24] H.K. Kim, J. Power Sources 162 (2006) 1232.
[25] Y. Yang, Y.C. Liang, J. Power Sources 165 (2007) 185.
[26] H. Yang, T.S. Zhao, Q. Ye, Electrochem. Commun. 6 (2004) 1098.
[27] W.W. Yang, T.S. Zhao, Electrochim. Acta 52 (2007) 6125.
[28] Z.H. Wang, C.Y. Wang, J. Electrochem. Soc. 150 (2003) A508.
[29] K. Scott, W. Taama, J. Cruickshank, J. Power Sources 65 (1997) 159.